

Magnetic phase diagram of  $\text{Fe}_{80-x}\text{Ni}_x\text{Cr}_{20}$  ( $10 \leq x \leq 30$ ) alloys

A. K. Majumdar\* and P. v. Blanckenhagen

*Kernforschungszentrum Karlsruhe, Institute für Angewandte Kernphysik I,  
Postfach 3640, D-7500 Karlsruhe, Federal Republic of Germany*

(Received 15 March 1983; revised manuscript received 19 October 1983)

Detailed magnetic measurements and a few neutron-diffraction experiments were performed on polycrystalline  $\text{Fe}_{80-x}\text{Ni}_x\text{Cr}_{20}$  alloys, with  $x=30, 26, 23, 21, 19, 17, 14,$  and  $10$ . All the alloys are fcc except the one with  $x=10$ , which is a mixture of fcc and bcc phases. The system is ferromagnetic for  $x=30$ . The alloys with  $x=26$  and  $23$  make transitions from a ferromagnetic to a Gabay-Toulouse ferromagnetic—spin-glass mixed phase at a lower temperature. Clear evidence of the presence of a spontaneous ferromagnetic bulk magnetization in this mixed phase supports recent theories predicting  $Z$  ferromagnetism and  $X$ - $Y$  spin-glass freezing. For  $x=21$  and  $19$  there is a spin-glass phase in low fields with some evidence of a field-induced ferromagnetism at high fields. Long-range antiferromagnetism takes over for the alloys with  $x=17, 14,$  and  $10$ . This sequence of compositional phase transition is due to competing ferromagnetic and antiferromagnetic interactions present in this system.

## I. INTRODUCTION

Magnetic materials having a random mixture of ferromagnetic and antiferromagnetic interactions have recently attracted a lot of attention. Fe-Ni binary alloys show around 35 at. % Ni Invar anomalies. This is due to the negative exchange integral of electrons of nearest-neighbor Fe atoms in an fcc lattice giving rise to antiferromagnetism of Fe in the fcc  $\gamma$  phase. It is not possible to study the antiferromagnetic  $\gamma$  phase of Fe below 1180 K due to the  $\gamma \rightarrow \alpha$  transformation. Addition of any one of Mn, Cr, or V stabilizes the  $\gamma$  phase and allows one to study in Fe-Ni alloys a complete transition region from antiferromagnetism (Fe rich) to ferromagnetism (Ni rich) within the same crystallographic fcc phase. Fe-Ni-Cr alloys are one such system where magnetic phase studies are very important in order to understand the magnetism of stainless steel. Many special properties of stainless and heat-resistant steels depend on their magnetic state.<sup>1</sup> Men'shikov *et al.*<sup>2</sup> had established qualitatively the ternary magnetic phase diagram of the Fe-Ni-Cr system through bulk magnetization and small-angle neutron scattering experiments. Figure 1 shows the ternary diagram, the dotted-dashed line separating the  $\gamma$  from the  $\alpha$  and other crystallographic phases of Fe-Ni-Cr alloys. The so-called "critical scattering" appears at those compositions for which the Curie temperature  $T_C$  is close to zero. The solid line for  $T_C=0$  is the critical concentration line and it separates the ferromagnetic (FM) phase from the paramagnetic (P) one. For alloys with  $[\text{Fe}] \geq 60$  at. % and  $[\text{Cr}] = 5-20$  at. % the low-field and the low-temperature dc magnetization showed some kind of anomalous peaks. However, the exact nature of this phase in this investigation remained more or less unexplored. In some other studies Men'shikov and Teplykh<sup>3</sup> and Nathans and Pickart<sup>4</sup> found no evidence of long-range antiferromagnetism from coherent neutron scattering at 4.2 K in polycrystalline  $\text{Fe}_{72}\text{Ni}_{17}\text{Cr}_{11}$ , (Ref. 3),  $\text{Fe}_{70}\text{Ni}_{15}\text{Cr}_{15}$  (Ref. 3),

and  $\text{Fe}_{71}\text{Ni}_{11}\text{Cr}_{18}$  (Ref. 4) (marked in Fig. 1). Therefore, it was concluded<sup>3</sup> that the antiferromagnetic order in stainless steel could only be of short range. However, Ishikawa *et al.*<sup>5,6</sup> detected long-range antiferromagnetism in a single crystal of  $\text{Fe}_{70}\text{Ni}_{15}\text{Cr}_{15}$  (Ref. 5) [analyzed composition  $\text{Fe}_{74}\text{Ni}_{15}\text{Cr}_{11}$  (Ref. 6), also shown in Fig. 1] with a Néel temperature  $T_N$  of 26 K.

The motivation behind the present work is to take only a few polycrystalline alloys (along the constant  $[\text{Cr}] = 20$  at. % line) of type  $\text{Fe}_{80-x}\text{Ni}_x\text{Cr}_{20}$  ( $10 \leq x \leq 30$ ) and find out the specific nature of magnetic phases at each stage as Ni concentration increases from 10 to 30 at. %. This will cover the hitherto unexplored region mentioned above as

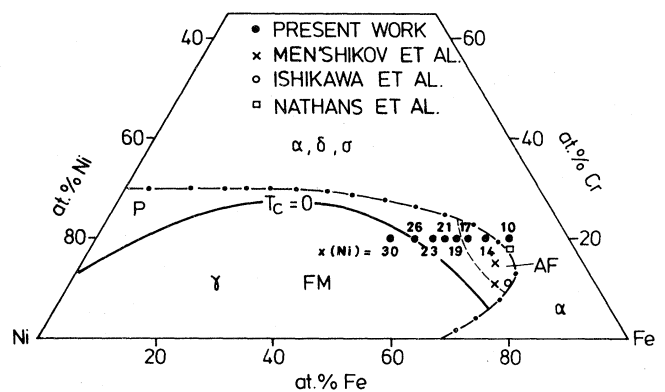


FIG. 1. Ternary diagram of FeNiCr system showing crystallographic and magnetic phases. The dotted-dashed line separates the  $\gamma$  phase from  $\alpha, \delta,$  and  $\sigma$  phases at room temperature. The solid line for  $T_C=0$  separates the ferromagnetic (FM) phase from the paramagnetic (P) one (Ref. 2). A tentative boundary between the paramagnetic and the antiferromagnetic (AF) phases is shown with a dashed line (present work). ●, present work; ×, Men'shikov *et al.* (Ref. 3); ○, Ishikawa *et al.* (Refs. 5 and 6); □, Nathans *et al.* (Ref. 4).

well as the stainless-steel composition where the presence of long-range antiferromagnetism is still an open question. For this purpose we have made bulk magnetization measurements as a function of field and temperature and a few neutron-diffraction measurements. We find a very clear evidence of (i) a long-range antiferromagnetism (AF) for alloys with  $x = 14$  and  $17$ , (ii) a spin-glass (SG) phase for  $x = 19$  and  $21$ , (iii) a double transition from paramagnetic (P)→ferromagnetic (FM)→mixed FM and SG phases having spontaneous moments for  $x = 23$  and  $26$ , and (iv) only a ferromagnetic phase for  $x = 30$ . Our high-field magnetization measurements also show some evidence of field-induced ferromagnetism (FIFM) in alloys with  $x = 19$  and  $21$  and this aspect was entirely missing in earlier studies.<sup>2,3</sup> Very similar phase diagrams have been recently found for  $\gamma$ -(Fe-Ni-Mn) alloys.<sup>7</sup> A double transition is also observed in many other systems, e.g.,  $(\text{Fe}_{1-x})_3\text{Al}_x$ ,<sup>8</sup>  $(\text{PdFe})_{1-x}\text{Mn}_x$ ,<sup>9</sup> ionic  $\text{Eu}_x\text{Sr}_{1-x}\text{S}$ ,<sup>10</sup> amorphous  $(\text{Fe}_x\text{Mn}_{1-x})_{75}\text{P}_{16}\text{B}_6\text{Al}_3$ ,<sup>11</sup> and  $\text{Fe}_x\text{Cr}_{1-x}$ .<sup>12</sup>

Many of the above data were interpreted in terms of the Sherrington and Kirkpatrick (SK) model<sup>13</sup> concerning Ising spins. This theory predicts a double transition  $P \rightarrow \text{FM} \rightarrow \text{SG}$ , but here the lowest temperature SG phase is a pure spin-glass and not a mixed FM and SG phase. Later Gabay and Toulouse,<sup>14</sup> taking isotropic vector spins (since experimental spins are Heisenberg-type), found a mixed phase where a spontaneous magnetization coexists with a spin-glass ordering of the transverse components of the spins. Recent data on Au-Fe (Ref. 15) support the above model. Villain<sup>16</sup> introduced a "semi-spin-glass" in which the ground-state configuration is a mixture of a Z ferromagnetic, antiferromagnetic, or ferrimagnetic spin component and an X-Y spin-glass component. Experimental data on the insulating compound  $\text{Co}_2\text{TiO}_4$  (Ref. 17) show a spin-glass behavior along with a nonvanishing spontaneous ferrimagnetic magnetization. Our observation of a spontaneous bulk ferromagnetism in the mixed phase (alloys with  $x = 26$  and  $23$ ) is only second to a similar one in Au-Fe.<sup>15</sup> The general features of the double transition are also in agreement with the above theories.<sup>14,16</sup>

## II. EXPERIMENTAL

Eight ternary  $\text{Fe}_{80-x}\text{Ni}_x\text{Cr}_{20}$  ( $10 \leq x \leq 30$ ) alloys with  $x = 10, 14, 17, 19, 21, 23, 26,$  and  $30$  were prepared by induction melting in an argon atmosphere. The starting materials were of 99.999% purity obtained from M/s Johnson Matthey Inc., England. Figure 1 shows the compositions of these alloys on the ternary diagram. They lie on the constant  $[\text{Cr}] = 20$  at. % line, which passes through both the stainless and heat-resistant steels' composition regions.<sup>1</sup> The alloys were cut to the required size, homogenized at  $1050^\circ\text{C}$  for 100 h in argon atmosphere, and then quenched in oil.

The magnetization was measured in all the samples, with the use of a computer-controlled Faraday balance with a superconducting magnet system (Oxford Instruments, United Kingdom), at each temperature in equilibri-

um down to 2 K and as a function of magnetic fields up to 60 kOe.<sup>18</sup> The absolute accuracy of the measured moment was typically 2%. However, the accuracy of the absolute value of the susceptibility in low fields is rather poor since the field value in the superconducting magnet is only roughly known at low fields, although it remains quite constant during measurements. In order to supplement the magnetization data we did neutron-diffraction measurements in alloys with  $x = 14, 17,$  and  $21$  as a function of temperature down to about 2 K, using the D1B spectrometer ( $\lambda = 2.518 \text{ \AA}$ ) at the Institut Laue-Langevin (Grenoble) high-flux reactor.

Chemical analysis of Ni and Cr shows that the compositions of the alloys are within  $\pm 0.5$  at. % of their nominal values. X-ray diffraction data at room temperature in powdered samples reveal that the alloys are single-phase fcc ( $\gamma$ ) with the lattice parameter  $a = 3.59 \text{ \AA}$  except for  $x = 10$ . This alloy is a mixture of two phases, bcc ( $\alpha$ ) with  $a = 2.88 \text{ \AA}$  and fcc ( $\gamma$ ) with  $a = 3.60 \text{ \AA}$ . The ratio of the two phases depends very much on the quenching rate as well as on cold working. Faster quenching produces more  $\gamma$  phases while cold work transforms the  $\gamma$  phase precipitates to the ferromagnetic  $\alpha$  phase. Neutron-diffraction data show that the alloys with  $x = 14, 17,$  and  $21$  are single-phase fcc ( $\gamma$ ) also down to 2 K.

## III. RESULTS AND DISCUSSIONS

### A. Alloy with $x = 30$

We find from the field and the temperature dependence of magnetization that the alloy  $x = 30$  is a spontaneous ferromagnet with a saturation magnetization  $4\pi M_s = 3.8$  kG. The Curie temperature  $T_C$ , found from the high-field magnetization isotherms (Arrott plots<sup>19</sup>), is  $\simeq 144$  K and differs somewhat from  $\simeq 100$  K as found from the ternary diagram given by Men'shikov *et al.*<sup>2</sup> The values of  $4\pi M_s$  and  $T_C$  are given in Table I.

The low-temperature magnetization  $M$  in the zero-field

TABLE I. Values of transition temperatures  $T_C$ ,  $T_{\text{SG}}$ ,  $T_N$ , and saturation magnetization  $4\pi M_s$  in  $\text{Fe}_{80-x}\text{Ni}_x\text{Cr}_{20}$  ( $10 \leq x \leq 30$ ) alloys.

Composition		$T_C$	$T_{\text{SG}}$	$T_N$	$4\pi M_s$
[Fe] (at. %)	[Ni] (at. %)	(K)	(K)	(K)	(kG)
50	30	144			3.8
54	26	56	7		1.92
57	23	35	20		0.69
59	21		10		
61	19		12		
63	17			13	
66	14			26	
70	10	> 300		40	3.7
		( $\alpha$ phase)		( $\gamma$ phase)	( $\alpha$ phase)

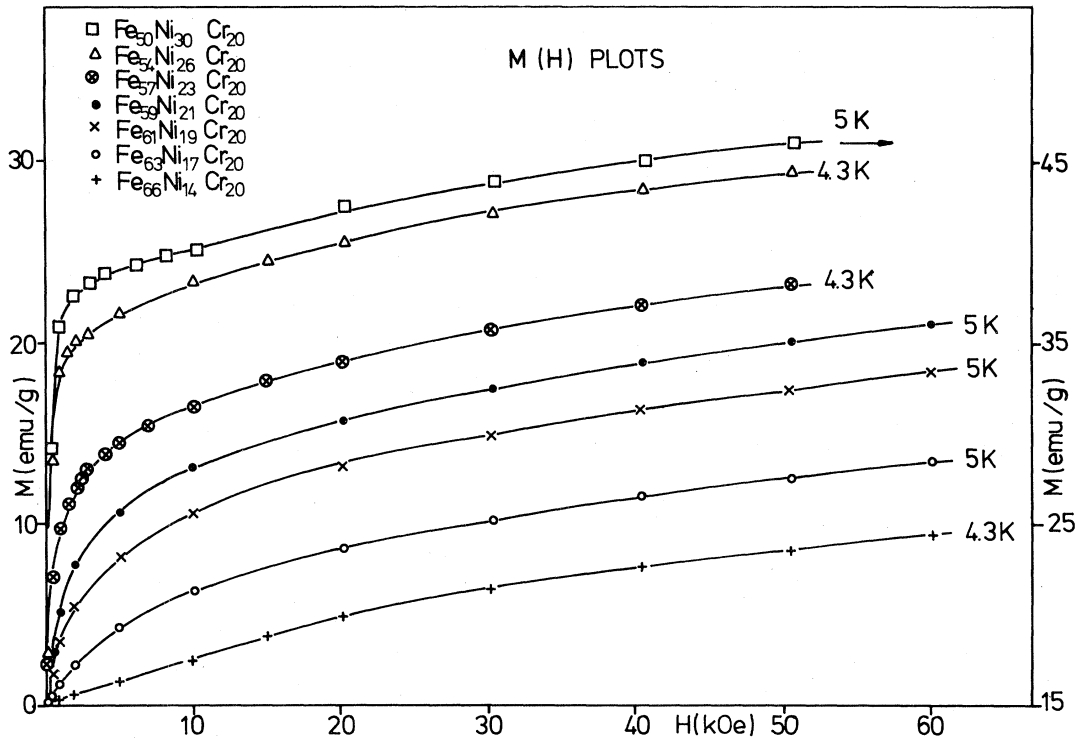


FIG. 2. Magnetization ( $M$ ) is plotted against external field ( $H$ ) at low temperatures for  $\text{Fe}_{80-x}\text{Ni}_x\text{Cr}_{20}$  alloys with  $x = 14, 17, 19, 21, 23, 26,$  and  $30$  (zero-field cooled).

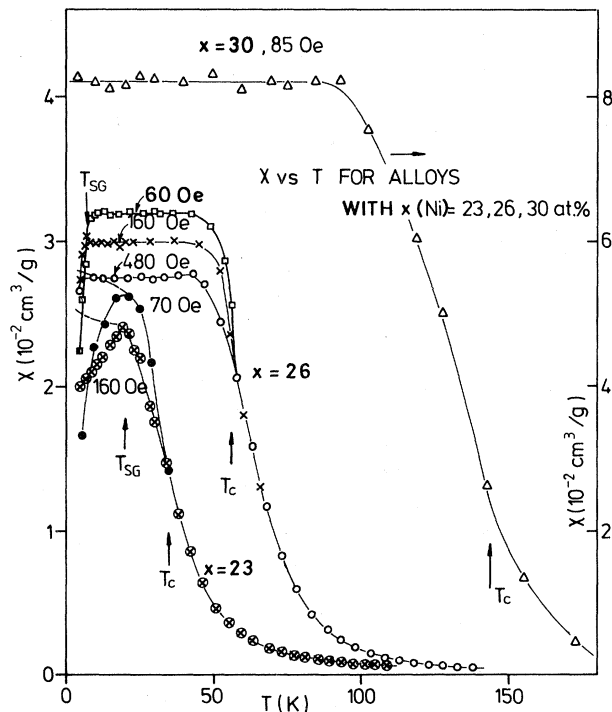


FIG. 3. Magnetic susceptibility ( $\chi$ ) vs temperature ( $T$ ) for  $\text{Fe}_{80-x}\text{Ni}_x\text{Cr}_{20}$  alloys with  $x = 30, 26,$  and  $23$  in external fields shown. The dashed curves show the effect of field cooling in the respective measuring fields for  $x = 23$ .

cooled state is plotted against the external magnetic field  $H$  in Fig. 2 for all the alloys under investigation except  $x = 10$ . All of them have a high-field susceptibility of about  $10^{-4} \text{ cm}^3/\text{g}$  at  $H = 50 \text{ kOe}$  and  $T = 4.2 \text{ K}$ . It is clear from this figure that the system gradually becomes ferromagnetic as Ni increases and consequently Fe decreases. More meaningful conclusions could be drawn from the low-field magnetization measurements. Figure 3 presents the low-field susceptibility  $\chi$  vs  $T$  for the alloys  $x = 30, \chi$  well below  $T_C$  (which is also found to be  $\approx 144 \text{ K}$  from the maximum of  $-\text{d}\chi/\text{d}T$  vs  $T$  plot) is constant due to demagnetization effects and shows that the ferromagnetic phase continues down to the lowest temperatures.

#### B. Alloys with $x = 26$ and $23$

Knowing the demagnetization factor for a spherical sample we find from the low-field  $M$ -vs- $H$  plots for  $x = 26$  and  $23$  at  $4.3 \text{ K}$  that they are spontaneous ferromagnets with  $4\pi M_s = 1.92$  and  $0.69 \text{ kG}$ , respectively. Arrott plots also give very similar  $4\pi M_s$  values. In Fig. 3 we see that for  $x = 26$  also  $\chi$  is demagnetization limited but at approximately  $7 \text{ K}$  there is a decrease of  $\chi$ , this decrease being more at lower fields and takes place at higher temperatures. This behavior is similar to that of a spin-glass. The system, on cooling, makes transitions from a paramagnetic ( $P$ ) to a ferromagnetic ( $FM$ ) to a mixed phase. The characteristic transition temperatures are  $T_C$  and  $T_{SG}$ , respectively.  $T_C$  is the temperature where  $\chi$  shows the sharpest increase with decreasing temperature

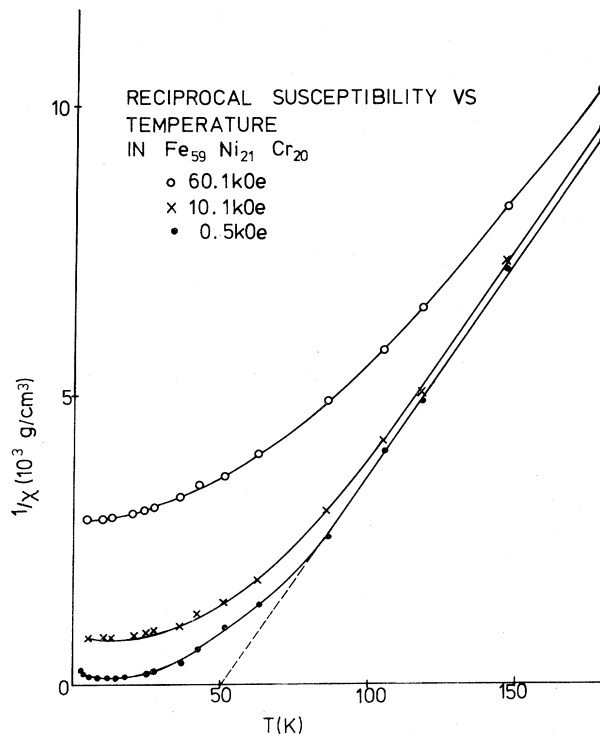


FIG. 4. Reciprocal susceptibility ( $1/\chi$ ) vs temperature ( $T$ ) for  $\text{Fe}_{59}\text{Ni}_{21}\text{Cr}_{20}$  at three external fields.

and is  $\approx 56$  K, while  $T_{\text{SG}} = 7$  K for the alloy  $x = 26$ . The values of  $T_C$  and  $T_{\text{SG}}$  are given in Table I. This low-temperature phase has many characteristics of a spin-glass, including the increase of  $\chi$  by field cooling below  $T_{\text{SG}}$ , as shown by the dashed curves for the alloy  $x = 23$  for example (Fig. 3), but the nature of this phase is still not clear without other supporting experiments, e.g., ac susceptibility, Mössbauer spectroscopy, etc. The alloy with  $x = 23$  also has a double transition, the two temperatures  $T_C = 35$  K and  $T_{\text{SG}} = 20$  K being quite close to each other. The identification of the  $P$ -FM transition in this alloy is difficult from an initial look at the  $\chi$ -vs- $T$  plot (Fig. 3). A spontaneous moment, found from the  $M$ -vs- $H$  plot, gave us evidence for the existence of this transition.

To summarize the data for the alloys with  $x = 26$  and 23, it is clear from the low-field  $M$ -vs- $H$  plots as well as Arrott plots at 4.3 K that the system retains its spontaneous moment even for  $T < T_{\text{SG}}$  (7 and 20 K, respectively). So the ground state is a mixed phase showing both ferromagnetic and spin-glass characteristics. This conclusion is amply supported by recent theories.<sup>14,16</sup>

### C. Alloys with $x = 21, 19$ , and 17

The alloys with  $x = 21, 19$ , and 17 have no spontaneous moment as found from  $M$ -vs- $H$  plots at lower fields. Figure 2 clearly shows that at low fields, even at the lowest temperatures, the magnetization increases much more slowly with field than that in a spontaneous ferromagnet (compare especially with alloys  $x = 26$  and 30 with sizable  $4\pi M_s$ ). A plot of the reciprocal susceptibility  $1/\chi$  vs  $T$  for  $x = 21$  is given in Fig. 4 for three values of external

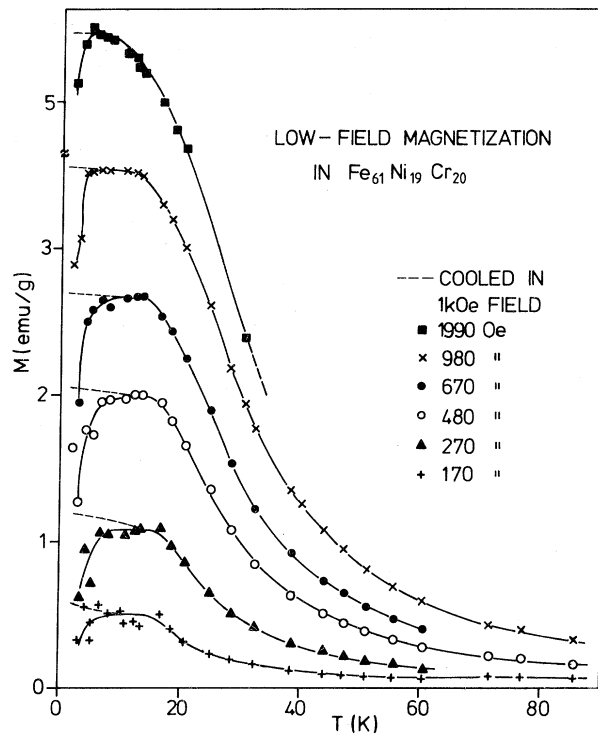


FIG. 5. Magnetization ( $M$ ) is plotted against temperature ( $T$ ) at several low fields in  $\text{Fe}_{61}\text{Ni}_{19}\text{Cr}_{20}$ . Dashed curves show the effect cooling in a field of 1 kOe.

field. It gives a Curie-Weiss behavior ( $H = 0.5$  kOe) from 80 K extending up to the highest temperature of our measurements. The effective moment considering all atoms, as calculated from the slope of the high-temperature straight line, is about  $2.5\mu_B$  per atom and is much larger than the saturation moment of  $\approx 0.2\mu_B$  per atom, found from Fig. 2. Alloys with  $x = 19$  and 21 also have similar behavior. The values of the moments and the deviations from linearity<sup>20</sup> (Fig. 4) for  $T \gg T_{\text{SG}}$  are similar in other spin-glasses.

In Fig. 5 we have plotted  $M$  vs  $T$  for the alloy  $x = 19$  (similar for  $x = 21$  and 17 also) at several values of low external fields. The following two procedures were used for this kind of low-field measurements. (i) The sample was cooled from room temperature down to 2 K in zero field. The magnetization was measured as a function of field. The sample was heated above 30 K and then cooled again to another temperature in zero field. The solid lines are through the data points taken in the zero-field cooled state.  $M$  increases with  $T$ , reaches broad maxima at around 12 K and then falls off rather sharply. This is typical of a long-range antiferromagnetic or a spin-glass. We got irreproducible results if we did not properly heat the sample well above the peak temperature. This kind of behavior is recently observed in the case of amorphous Fe-Mn alloys.<sup>11</sup> (ii) The sample was cooled down from above 30 K in a field (1 kOe for alloy  $x = 19$ ), the magnetization was measured at various fields and then the temperature was raised to a new value. The dashed curves of Fig. 5 show that the peaks are smoothed out in the field-

cooled state. This thermomagnetic-history dependence, however, is a characteristic feature of a spin-glass freezing. In all the three alloys we find that the broad peaks in  $M$  gradually disappear at higher fields. This critical field increases with higher Fe content, viz., it is about 2 kOe for  $x = 21$  but about 5 kOe for  $x = 17$ . This is due to the fact that the presence of more Fe prevents the spin-glass phase from being disrupted easily by the external fields.

Neutron scattering is the best experimental tool to distinguish between these two possible low-temperature phases, viz., spin-glass and antiferromagnetic. Our neutron-diffraction studies<sup>21</sup> in the alloy  $x = 17$  show rather weak but sharp superstructure (110) peaks at low temperatures from which the Néel temperature  $T_N$  could be roughly estimated to be around 10 K. Nevertheless, the peak width yields a correlation length of more than 300 Å. The intensity of the (110) peak at 2.2 K decreased considerably above 5 kOe when measured as a function of field, in good agreement with the magnetization data. No magnetic coherent scattering could be observed in the alloy  $x = 21$  down to 2.5 K. Thus we conclude that  $x = 21$  may be spin-glass whereas  $x = 17$  is antiferromagnetic. But the alloy  $x = 17$  also shows the characteristics of a spin-glass in our magnetization measurements (field cooling). This is not clear to us. However, this may be possible if there is another transition at a lower temperature to a mixed antiferromagnetic–spin-glass state. There is a place for such a mixed phase in the model of Villain<sup>16</sup> on the antiferromagnetic side just as we have observed a mixed phase on the ferromagnetic side for  $x = 26$  and 23. If the two transition temperatures  $P \rightarrow \text{AF} \rightarrow \text{mixed}$  ( $\text{AF} + \text{SG}$ ) are quite close, magnetization measurements will not be able to resolve them. Small-angle neutron scattering may

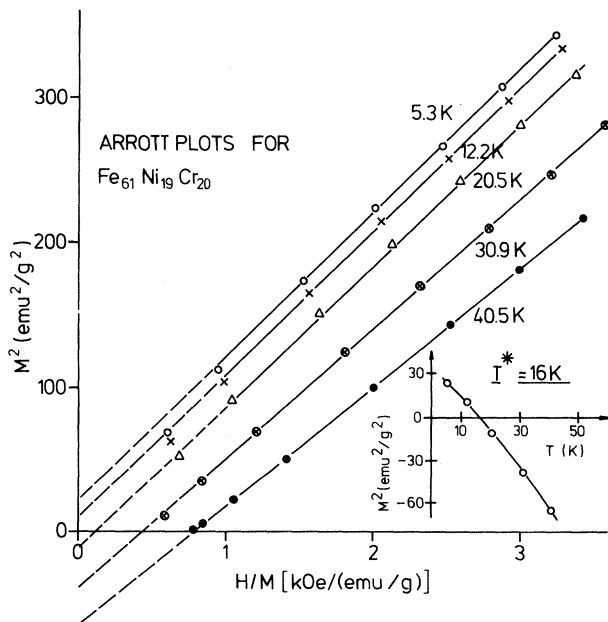


FIG. 6. Arrott plots ( $M^2$  vs  $H/M$ ) at several temperatures to show evidence for field-induced ferromagnetism in  $\text{Fe}_{61}\text{Ni}_{19}\text{Cr}_{20}$ . The inset gives  $T^* = 16$  K.

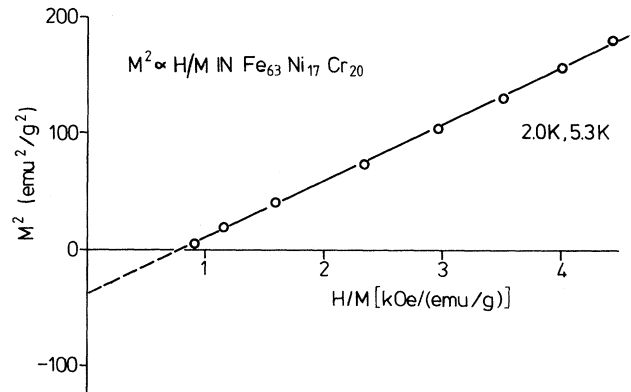


FIG. 7. Arrott plot ( $M^2$  vs  $H/M$ ) at 2.0 and 5.3 K (identical curve for both temperatures) for  $\text{Fe}_{63}\text{Ni}_{17}\text{Cr}_{20}$  showing no evidence of field-induced ferromagnetism.

presumably be able to detect such a transition to the mixed phase by showing a “critical scattering” due to spin-glass freezing.

The magnetic state of the alloys with  $x = 21$  and 19 seems to be more complicated than that of a spin-glass when we take a close look at the high-field data. In Fig. 6 we have plotted  $M^2$  against  $H/M$  at various temperatures (Arrott plots<sup>19</sup>) for the alloy  $x = 19$ . The data above 20 kOe fall on a set of nearly parallel straight lines having positive intercepts on the  $M^2$  axis at low temperatures, suggesting field-induced ferromagnetism (FIFM). These intercepts plotted against temperature (inset of Fig. 6) yield a characteristic temperature  $T^* = 16$  K for  $x = 19$ .  $T^*$  should not be identified with a critical temperature. For  $T < T^*$  and at lower fields the curves bend towards the origin, showing no spontaneous magnetization. Low-field  $M$ -vs- $H$  data also show the absence of spontaneous moment. Similarly, we get  $T^* = 33$  K for  $x = 21$ . This might imply that the alloys with  $[\text{Ni}] = 21$  and 19 make a transition from a low-field spin-glass state (no spontaneous moment) to a field-induced ferromagnetic one at higher fields. This observation of a field-induced ferromagnetism was entirely missing in the work of Men'shikov *et al.*<sup>2</sup> Another Arrott plot is shown in Fig. 7 for the alloy  $x = 17$ . Here we find that the intercept is negative even at 2 K, indicating the absence of field-induced ferromagnetic ordering. This is not unexpected. This alloy is too poor in Ni to support even field-induced ferromagnetism.

#### D. Alloy with $x = 14$

The magnetic susceptibility of the alloy  $x = 14$  is presented in Fig. 8 at a few external fields both in the zero-field and the field cooled states. There are well-defined peaks typical of an antiferromagnet at  $T = (26 \pm 1)$  K at lower fields. The data at 30 kOe show no special feature. The peak temperature shifts slightly to higher values at lower fields. The coherent neutron scattering<sup>21</sup> also gives clear evidence of long-range antiferromagnetism in this alloy with  $T_N = (30 \pm 10)$  K, and the lower limit of

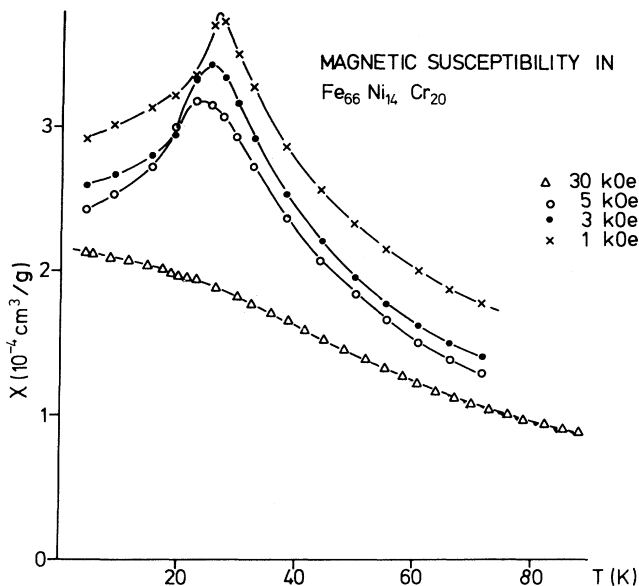


FIG. 8. Magnetic susceptibility ( $\chi$ ) vs temperature ( $T$ ) for  $\text{Fe}_{66}\text{Ni}_{14}\text{Cr}_{20}$  at several external fields.

the correlation length is estimated to be about 300 Å. Thus we were able to definitely establish the presence of long-range antiferromagnetism in polycrystalline samples of Fe-Ni-Cr alloy around the stainless-steel composition (our alloys with  $x = 14$  and 17), in contrast to those of Men'shikov and Teplykh<sup>3</sup> and Nathans and Pickart.<sup>4</sup> Our studies therefore confirm the single-crystal data of Ishikawa *et al.*<sup>5,6</sup> We show in Fig. 1 the boundary between the paramagnetic ( $P$ ) and the antiferromagnetic ( $AF$ ) phases by a dashed line tentatively derived from the above studies.

We find from the discussions of Secs. III C and III D that the alloys with  $x = 21, 19, 17,$  and  $14$  make compositional phase transitions from a spin-glass to a long-range antiferromagnetic state, and this is clearly due to a decrease in the overall ferromagnetic interaction (see Sec. IV for more detailed discussion). The magnetic susceptibilities in these alloys at  $H = 1$  kOe and  $T = T_{SG}$  or  $T_N$  are  $(80, 50, 13,$  and  $4) \times 10^{-4} \text{ cm}^3/\text{g}$ , respectively. It is generally found<sup>7</sup> that  $\chi$  of spin-glasses is about an order of magnitude higher than that of an antiferromagnet. Our values therefore show that this compositional phase transition is only gradual.

#### E. Alloy with $x = 10$

Finally in an alloy with  $x = 10$  we find that the magnetization ( $M$ ) has a peak around 40 K and then it hardly decreases with increasing temperature up to 300 K. The  $M$ -vs- $H$  curve at 4 K gives  $4\pi M_s = 3.7$  kG. This alloy is a mixture of two phases. The peak in  $M(T)$  is most probably due to the antiferromagnetic fcc  $\gamma$ -Fe with  $T_N = 40$  K, and the high-temperature ferromagnetic phase ( $T_C > 300$  K) is due to the bcc  $\alpha$  phase. The Néel temperature of  $\gamma$ -Fe was already found to be around 40 K from Mössbauer measurements<sup>22</sup> in  $\text{Fe}_{71}\text{Ni}_9\text{Cr}_{20}$  and sus-

ceptibility data<sup>23</sup> in  $\text{Fe}_{73}\text{Ni}_9\text{Cr}_{18}$ , which are very similar in composition to our alloy  $x = 10$ . Also, Rode *et al.*<sup>24</sup> had shown that a composition of 10% by volume of  $\gamma$  phase is quite sufficient to demonstrate the "latent" antiferromagnetism in Fe-rich alloys.

#### IV. CONCLUSIONS

It is quite clear from the earlier sections that as one increases Ni content  $x$ , the system makes a compositional phase transition from a long-range antiferromagnetic phase to a long-range ferromagnetic one, passing through interesting intermediate phases. This sequence could be qualitatively understood in terms of pair exchange integrals of the components Fe, Ni, and Cr. From inelastic small-angle neutron-scattering, Men'shikov *et al.*<sup>25</sup> estimated the pair exchange integrals in  $I(\text{Fe-Fe}) = -7$  meV,  $I(\text{Ni-Ni}) = 52$  meV,  $I(\text{Cr-Cr}) = -227$  meV,  $I(\text{Fe-Ni}) = 36$  meV,  $I(\text{Fe-Cr}) = 39$  meV, and  $I(\text{Ni-Cr}) = 122$  meV. Since Cr concentration remains unchanged and Ni concentration increases at the cost of Fe concentration,  $I(\text{Cr-Cr})$  and  $I(\text{Fe-Ni})$  will have more or less the same effect on the magnetic ordering of these alloys. The addition of the other integrals gradually makes the system more ferromagnetic as  $x$  increases.

In conclusion we present in Fig. 9 a magnetic phase diagram of the  $\text{Fe}_{80-x}\text{Ni}_x\text{Cr}_{20}$  system ( $10 \leq x \leq 30$ ) based on our discussions on individual alloys (Sec. III). At the highest Ni concentration ( $x = 30$ ), the system is an fcc ferromagnet (FM). As Ni content decreases for  $x = 26$  and 23 the system enters from a long-range ferromagnetic state to a mixed (FM + SG) one as the temperature is lowered. For  $x = 21, 19$  the system is too poor in Ni to support long-range ferromagnetism at any temperature and shows characteristics of only a spin-glass (SG). This region is really in between long-range ferromagnetically and antiferromagnetically ordered regions. However, at

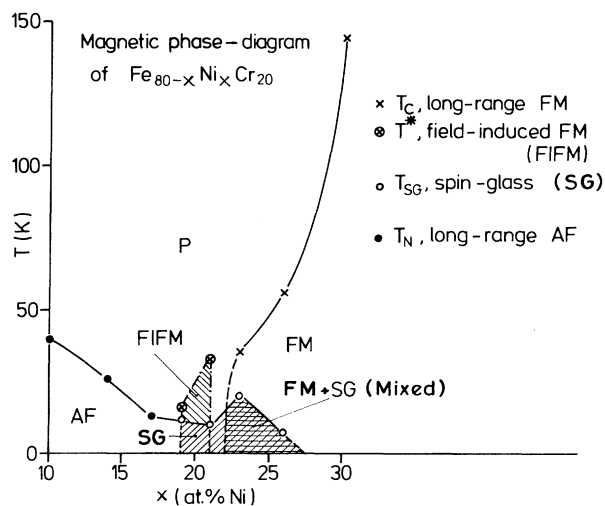


FIG. 9. Temperature ( $T$ ) vs Ni concentration ( $x$  in units of at.%) magnetic phase diagram of  $\text{Fe}_{80-x}\text{Ni}_x\text{Cr}_{20}$  alloys ( $10 \leq x \leq 30$ ).

fields above 20 kG we have some evidence of field-induced ferromagnetism (FIFM). As Ni content further decreases in alloys with  $x = 17$  and 14 (around the stainless and heat-resistant steels' composition), evidence of long-range antiferromagnetism (AF) is quite clear. For the alloy with  $x = 10$ , the  $\gamma$  phase is antiferromagnetic while the  $\alpha$  phase is bcc ferromagnetic.

Also according to our investigation the intersection of the  $T_C = 0$  curve with the line of constant  $[\text{Cr}] = 20$  at. % is at around  $[\text{Fe}] = 58$  at. %. This is to be contrasted with the value of  $[\text{Fe}] = 53$  at. % found by Men'shikov *et al.*,<sup>2</sup> as shown in Fig. 1. Bendick and Pepperhoff<sup>26</sup> had found  $[\text{Fe}] \approx 60$  at. % as the critical concentration from Mössbauer spectroscopy.

*Note added in proof.* Recently, A. Mookerjee and S. B. Roy [J. Phys. F **13**, 1945 (1983)], using a different mean-

field approach, showed the existence of such a mixed phase in the Au-Fe alloy. The magnetic phase diagram of Au-Fe obtained by them is in good agreement with the available experimental phase diagram.

#### ACKNOWLEDGMENTS

The authors would like to acknowledge B. Scheerer for careful preparation of the alloys, V. Oestreich and D. Weschenfelder for help during the magnetic measurements, and D. Chowdhuri and S. B. Roy for many useful discussions. One of us (A.K.M.) also acknowledges the Alexander von Humboldt Foundation for financial support and Professor Dr. W. Schmatz and Dr. G. Czjzek for their keen interest in the work.

\*On leave of absence from the Department of Physics, Indian Institute of Technology, Kanpur 208016, India.

- <sup>1</sup>R. M. Bozorth, in *Ferromagnetism* (van Nostrand, Princeton, New Jersey, 1951), p. 148.
- <sup>2</sup>A. Z. Men'shikov, S. K. Sidorov, and A. Ye. Teplykh, Phys. Met. Metallogr. (USSR) **45**, 42 (1979).
- <sup>3</sup>A. Z. Men'shikov and A. Ye. Teplykh, Phys. Met. Metallogr. (USSR) **44**, 78 (1979).
- <sup>4</sup>R. Nathans and S. J. Pickart, J. Phys. Chem. Solids **25**, 183 (1964).
- <sup>5</sup>Y. Ishikawa, Y. Endoh, and T. Takimoto, J. Phys. Chem. Solids **31**, 1225 (1970).
- <sup>6</sup>Y. Ishikawa, M. Kohgi, and Y. Noda, J. Phys. Soc. Jpn. **39**, 675 (1975).
- <sup>7</sup>A. Z. Men'shikov, P. Burlet, A. Chamberod, and J. L. Tholence, Solid State Commun. **39**, 1093 (1981).
- <sup>8</sup>R. D. Shull, H. Okamoto, and P. A. Beck, Solid State Commun. **20**, 863 (1976).
- <sup>9</sup>B. H. Verbeek, G. J. Nieuwenhuys, H. Stocker, and J. A. Mydosh, Phys. Rev. Lett. **40**, 586 (1978).
- <sup>10</sup>H. Maletta and P. Convert, Phys. Rev. Lett. **42**, 108 (1979).
- <sup>11</sup>Y. Yeshurun, M. B. Salamon, K. V. Rao, and H. S. Chen, Phys. Rev. Lett. **45**, 1366 (1980).
- <sup>12</sup>S. M. Shapiro, C. R. Fincher, Jr., A. C. Palumbo, and R. D. Parks, Phys. Rev. B **24**, 6661 (1981).
- <sup>13</sup>D. Sherrington and S. Kirkpatrick, Phys. Rev. Lett. **35**, 1792 (1975).
- <sup>14</sup>M. Gabay and G. Toulouse, Phys. Rev. Lett. **47**, 201 (1981).
- <sup>15</sup>F. Varret, A. Hamzić, and I. A. Campbell, Phys. Rev. B **26**, 5285 (1982).
- <sup>16</sup>J. Villain, Z. Phys. B **33**, 31 (1979).
- <sup>17</sup>J. Hubsch and G. Gavoille, Phys. Rev. B **26**, 3815 (1982).
- <sup>18</sup>A. K. Majumdar, V. Oestreich, D. Weschenfelder, and F. E. Luborsky, Phys. Rev. B **27**, 5618 (1983).
- <sup>19</sup>A. Arrott, Phys. Rev. **108**, 1394 (1957); A. Arrott and J. E. Noakes, Phys. Rev. Lett. **19**, 786 (1967).
- <sup>20</sup>A. F. J. Morgownik and J. A. Mydosh, Phys. Rev. B **24**, 5277 (1981); A. K. Majumdar, V. Oestreich, and D. Weschenfelder, Solid State Commun. **45**, 907 (1983).
- <sup>21</sup>A. K. Majumdar and P. V. Blanckenhagen, J. Magn. Mater. (to be published).
- <sup>22</sup>U. Gonser, C. J. Meehan, A. H. Muir, and H. Wiedersich, J. Appl. Phys. **34**, 2373 (1963).
- <sup>23</sup>E. I. Kondorsky and V. L. Sedov, J. Appl. Phys. **31**, 331 S(1960).
- <sup>24</sup>V. E. Rode, A. V. Deryabin, and G. Damashke, IEEE Trans. Magn. **MAG-12**, 404 (1976).
- <sup>25</sup>A. Z. Men'shikov, N. N. Kuz'min, V. A. Kazantsev, S. K. Sidorov, and V. N. Kalinin, Phys. Met. Metallogr. (USSR) **40**, 174 (1975).
- <sup>26</sup>W. Bendick and W. Pepperhoff, J. Phys. F **11**, 57 (1981).